An analytical expression
for the D.I.P.–P.I.P. flexion interdependence
in human fingers

KOOS JAAP VAN ZWIETEN[1]*, KLAUS P. SCHMIDT[1], GEERT JAN BEX[2],
PETER L. LIPPENS[1], WIM DUYVENDAK[3]

[1] Department of Anatomy, Morphology, BioMed Institute, University of Hasselt, Hasselt, Belgium.
[2] Database and Theoretical Computer Sciences Research Group, University of Hasselt, Hasselt, Belgium.
[3] Department of Neurosurgery, Jessa Hospital Hasselt, Hasselt, Belgium.

Empirical evidence shows that a strong correlation exists between the flexion angles of the distal and proximal interphalangeal (D.I.P., P.I.P.) joints of the human finger. Several authors measured this functional dependence, stating that the interdependence of D.I.P. and P.I.P. flexion is different for healthy individuals and patients displaying pathologies. The purpose of our study is to find an analytical expression for this correlation. Methods: Following closely the anatomical in situ relations, we developed a two-dimensional kinematical model which expresses analytically the D.I.P.–P.I.P. angle correlation. Numerical values for the model were extracted from one healthy and one pathological case data set. Results: The analytical form of the model allows for any P.I.P. angle not only to calculate the corresponding D.I.P. angle, but after first order differentiation with respect to the P.I.P. angle, it also shows the rate of change of the D.I.P. flexion. The model reproduces well the differences in the angular correlation of D.I.P. flexion of the two healthy-pathological data sets. Displaying the rate of change of D.I.P. flexion versus P.I.P. flexion provides an additional, clear-cut discriminatory tool between normal and pathological states. Conclusions: Information on differences between normal and pathological flexion of fingers is more pronounced and easier accessible from the derivatives of the D.I.P.–P.I.P. flexion behaviour than from direct angular correlation data. The analytical form of our model allows one to establish the rate of change of the D.I.P. angles, resulting in a better analysis of the situations at hand.

Key words: *model, finger, kinematical, interphalangeal, flexion, coordination*

1. Introduction

Some clinicians feel the need to investigate the correlation between the flexion ranges of the different finger joints for a clear distinction between a healthy and a pathological finger. When investigating the interrelation of quantities in different (e.g., healthy and pathological) cases, it is often more instructing, not to compare the direct change of the involved quantities, but to compare their rate of change, expressed by the first order derivative. Empirical evidence shows that a strong correlation exists between the flexion angles of the distal interphalangeal (D.I.P.)

and the proximal interphalangeal (P.I.P.) joint (e.g., [1]). This correlation, about which most authors agree, was experimentally quantified in the fingers of healthy individuals by Hahn et al. [7] and confirmed by Holguín et al. [9]. Consequently, the aim of our study is to find an analytical expression for this correlation, and to establish its first order derivative for better interpretation.

By different pathologies the interdependence in the flexion angles can be changed compared to the normal finger. In order to facilitate the evaluation of the current state of the finger we propose to model the involved flexion angle interdependence. Therefore we develop, starting from anatomy and actual measure-

ments, a mathematical model giving an analytical expression for the D.I.P.–P.I.P. angular correlation. Calculating and plotting its first-order derivative with respect to the independent flexion angle then improves the presentation of different situations and leads to a clearer tracing and recognition of anomalies.

2. Method

2.1. Anatomy of the finger, extensor aspect

The extensor assembly (dorsal aponeurosis, extensor apparatus) of the human finger consists of tendon fibers from the extensor digitorum muscle and the intrinsic hand muscles viz. the interosseus muscles and lumbrical muscle. Ligamentous fibers also join the extensor assembly. The proximal interphalangeal (P.I.P.) and the distal interphalangeal (D.I.P.) joint of the finger are extended by the extensor assembly, and flexed by tendons from respectively flexor digitorum superficialis muscle and flexor digitorum profundus muscle.

The extensor assembly of the finger

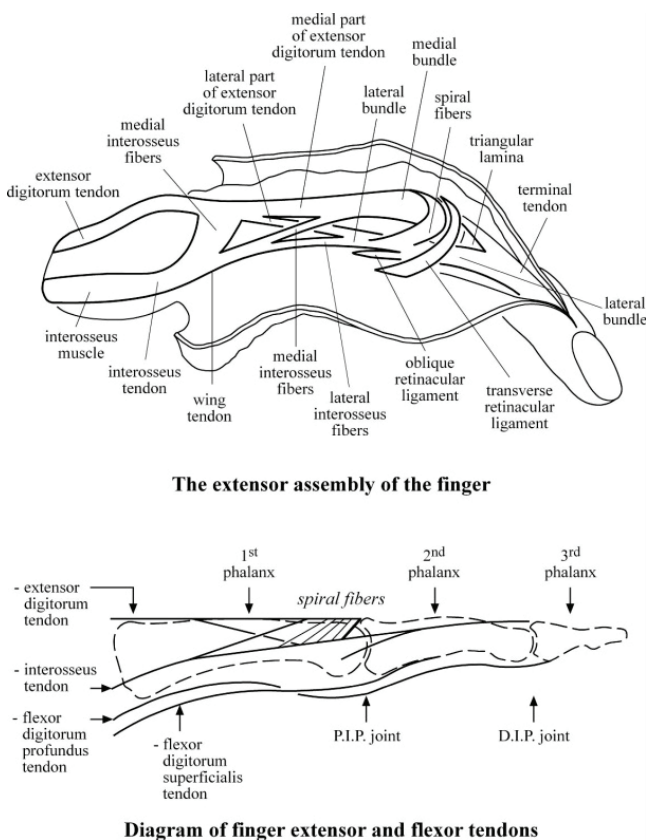

Diagram of finger extensor and flexor tendons

Fig. 1. Extensor assembly and diagram
of extensor and flexor tendons of the finger

Figure 1 gives above the details of extensor and flexor tendons of an anatomical specimen of the finger, ulnar aspect, after removal of skin and subcutaneous tissues. Below a lateral view represents the schematized sagittal plane. The most distal spiral fiber is indicated by a somewhat bolder line. See also Van Zwieten et al. [22].

Whereas the medial bundle of the extensor assembly runs over the dorsum of the proximal interphalangeal joint, the two lateral bundles of both sides pass the dorso-lateral aspect of this joint, to fuse more distally into one terminal tendon. This terminal tendon, however, runs dorsally over the distal interphalangeal joint, independent of its flexion angle. The spiral fibers of the extensor assembly of the finger, over the distal part of the first phalanx and at proximal interphalangeal (P.I.P.) joint level, connect the lateral bundles or side bands of the extensor assembly on either side of the finger with its medial bundle or central band. Interposed between central band and side bands at the insertion of the central band on the P.I.P. joint, these spiral fibers were sufficiently described by Hauck [8], Landsmeer [10], Van Zwieten [20], [21], Tubiana [16], [17], Zancolli and Cozzi [24], Tubiana et al. [18].

The whole complex of tendinous spiral fibers is currently held responsible for limiting the palmar displacements of the lateral bands during flexion of the P.I.P. joint [16]–[18], [20]–[22].

2.2. Kinematical model of D.I.P.–P.I.P. flexion

The foregoing survey shows that the anatomy of the finger is rather complex. However, in order to find the correlation between the two flexion angles, we established a simplified kinematical model based on the major parameters governing the flexion. In this kinematical model, tendons and tendon fiber bundles in a given finger are supposed to be symmetrical with respect to its length axis and to behave as inelastic, non-extensible wires of a given length. A line defined by the straight dorsum of the middle phalanx gives the reference from where the flexion angles θ (P.I.P. flexion) and φ (D.I.P. flexion) are measured. This is shown in a lateral view in Fig. 2.

During distal interphalangeal flexion simultaneously with proximal interphalangeal flexion, the medial as well as the lateral bundles are located in a sagittal plane [23]. Representing the finger in a lateral view in the next analyses is therefore justified.
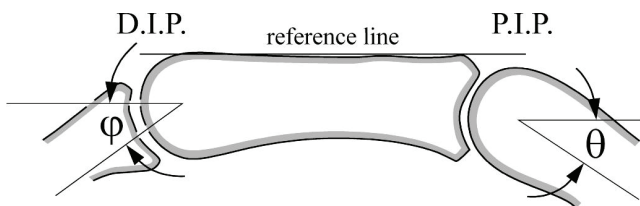
Fig. 2. Definition of the D.I.P.–P.I.P. flexion angles

The model of the finger flexion, the definition of all parameters, and the mathematical derivation of the analytical expression for the angular dependence of the finger flexion are given in detail in the Appendix. From the model we derived an analytical mathematical functional relation between the D.I.P.–P.I.P. flexion angles. The P.I.P. angle is arbitrarily chosen as the independent variable, the D.I.P. angle as the dependent one. For any given P.I.P. angle θ equation (1) calculates the corresponding D.I.P. angle φ.

$$\varphi(\theta) = \frac{\sqrt{a_x(0)^2 + a_y(0)^2} + s(0) - \sqrt{a_x(\theta)^2 + a_y(\theta)^2} - s(\theta)}{R(\theta)} \cdot$$

(1)

The model parameters a_x, a_y are connected to the interphalangeal distance d and the length of the most distal, terminal spiral fiber s. For modelling namely, it suffices to consider this terminal spiral fiber, as all the other spiral fibers are coupled to it and will behave analogously. The radius of curvature of the distal end of the middle phalanx is denoted as R. Except the distance d, all other parameters depend on the independent variable θ.

In order to get numerical expressions, the model was applied to two experimental data sets, one set for a (normal) intrinsic-plus finger (V+), the other for a (pathological) intrinsic-minus (V–) finger. Data were derived from one randomly chosen patient with a V intrinsic-minus finger (crosses in Fig. 4), due to unilateral ulnar palsy by ulnar nerve compression at one elbow [11], described by Van Zwieten et al. [23] From his non-affected hand the normal data were obtained (crosses in Fig. 3). For both data sets the phalangeal distance d was assumed as $d = 40$ mm [12], the initial angle of the terminal spiral fibers was assumed as $\alpha_0 = 10°$ [21]. Data were directly derived from angles, measured on video stills of healthy and ulnar-minus fingers in this patient, acquired under standard conditions by the use of techniques and methodologies recently described by Hahn et al. [7].

Only with an explicit analytical expression for the angle dependent spiral fiber length s and the radius of curvature R of the distal end of the middle phalanx, can equation (1) be used to describe the experimental

data in an analytical form. We therefore used equation (1) to evaluate D.I.P. angles $\varphi = \varphi(\theta)$ for 25 different P.I.P. angles θ, which covered equidistantly the experimental data range, and with such assumed numerical values for s and R, that the outcome would fit into the observed angular correlation pattern. The required numerical values for fiber length s and radius R were at each angle θ separately adjusted manually and empirically and in accordance with anatomical data, until the resulting coordinate pair $\varphi = \varphi(\theta)$ would reasonably fit into the given observed data.

This resulted in two discrete data sets of 25 numerical values for both the radius of curvature R and the terminal spiral fiber length s as a function of angle θ. Both the radius R and the terminal spiral fiber length s were then expressed by the 6th degree polynomial functions in the variable θ, approximating by least squares fits the empirical data series in radius R and fiber length s. Inserting the polynomial representation of the radius R and the fiber length s into equation (1) resulted in an overall analytical expression $\varphi = \varphi(\theta)$ for the functional dependence of the D.I.P. angle φ on the P.I.P. angle θ. The validity of the procedure is justified by the final result of the calculated angular correlations, shown by the full lines in Fig. 3 and Fig. 4.

The angular dependence of the radius of curvature $R(\theta)$ of the D.I.P. joint was assumed to be equal for both cases V+ and V–. The same behaviour of the radius of curvature R for both cases can be justified, because in a first-order approximation, the radius (although belonging to either data set) cannot be the cause of the difference between a normal and an ulnar palsy finger. The model joint curvature, starting from $R = 4$ mm for $\theta = 0°$, and first slightly decreasing with increasing P.I.P. angle, had to be increased by about 33% at $\theta = 120°$ in order to fit the data set. Arguments for this are the following. During 90° flexion of the P.I.P. joint, which is not a pure hinge joint, Dumont et al. [4] measured an increase of 30% of R of the head of the first phalanx in the sagittal plane. Although for the D.I.P. joint such data are not yet available, we may rely on the statements by Schmidt and Lanz [14] and Zumhasch et al. [25] that the form of the head of the second phalanx mimics that of the first phalanx, presuming a similar increase of R in the D.I.P. joint. So, our numerical data of radius R are in agreement with current anatomical data on the curvature of the D.I.P. joint.

When adjusting the length variation for the spiral fiber s, different results were obtained for the two data sets V+ and V–.

For V+ the model length of the lateral part of the terminal spiral fiber had to be shortened nearly linearly from the initial value of $s(0) = 4$ mm to 65% for $\theta = 120°$. The phenomenon of apparent shortening of a given spiral fiber during P.I.P. flexion is currently observed in normal anatomical specimens [21] under in vitro standard conditions (i.e., from strictly lateral views) comparable to the ones in the normal intrinsic plus finger in vivo [2]. The diverging of the condyles, over which distal spiral fibers run during P.I.P. flexion, creates an up-heaving, and thus shortening effect for such fibers in particular [21].

For V− the empirical length of the terminal spiral fiber with the initial value $s(0) = 4$ mm, slightly decreased during the first 60° and had to be increased by 45% towards $\theta = 120°$.

Such a late increase of a given spiral fiber in a finger with intrinsic weakness may be the result of altered interosseus muscle elasticity compared to the normal state [3]. The resulting effect on lateral bands and spiral fibers in intrinsic weakness was noticed earlier by Van Der Meulen [19]. In the normal finger such increase apparently does not occur.

3. Results

For reasons of simplicity, the final numerical expressions of equation (1) for the V− and V+ cases are omitted here, but instead the resulting graphs together with the experimental data are shown in Fig. 3 (V+) and Fig. 4 (V−). The analytical curves follow in an S-shape behaviour the measured D.I.P. = f(P.I.P.) angle values.
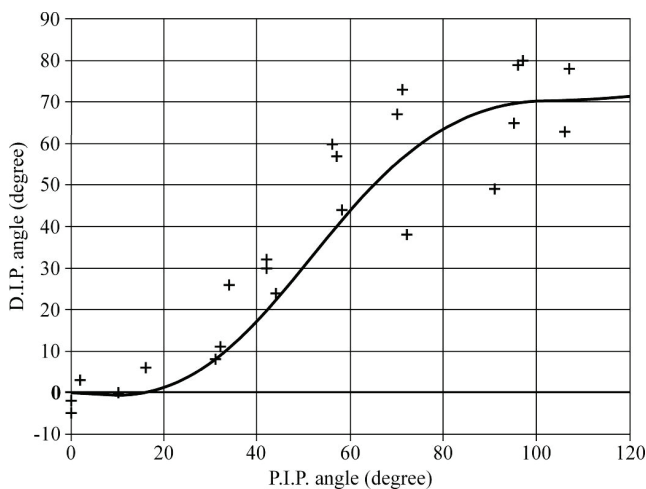

Fig. 3. Experimental data (crosses) and analytical fit (line) of D.I.P.–P.I.P. flexion angles for a V-plus finger
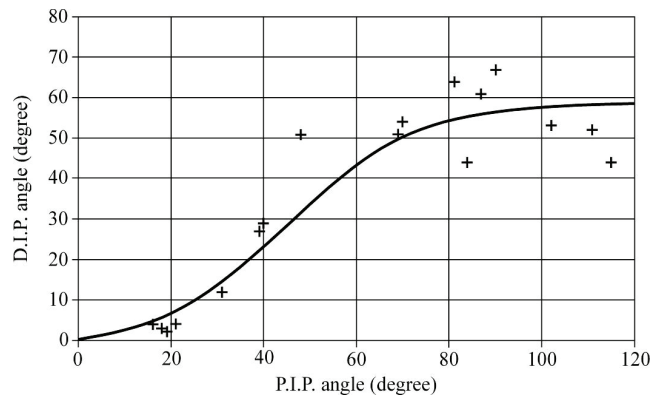

Fig. 4. Experimental data (crosses) and analytical fit (line) of D.I.P.–P.I.P. flexion angles for a V-minus finger

Display of the differences for a normal and a pathological behaviour in the correlation pattern between the P.I.P. and D.I.P. flexion angle is enhanced by calculating the first-order derivatives $\varphi' = \dfrac{d\varphi}{d\theta}$ of equation (1) for both cases. This was done by the technical computing software "Maple"® (http://www.maplesoft.com/). The mathematical derivative of equation (1) with respect to the angle θ gives the rate of change of the D.I.P. angle, i.e., the amount of D.I.P. flexion angle per unit P.I.P. flexion angle for all P.I.P. flexion angles. The final analytical expressions of the derivative of equation (1) with respect to the angle θ in their numerical forms for the V− and V+ cases are omitted here, but the resulting graphs for the cases V plus and V minus can be seen in Fig. 5.
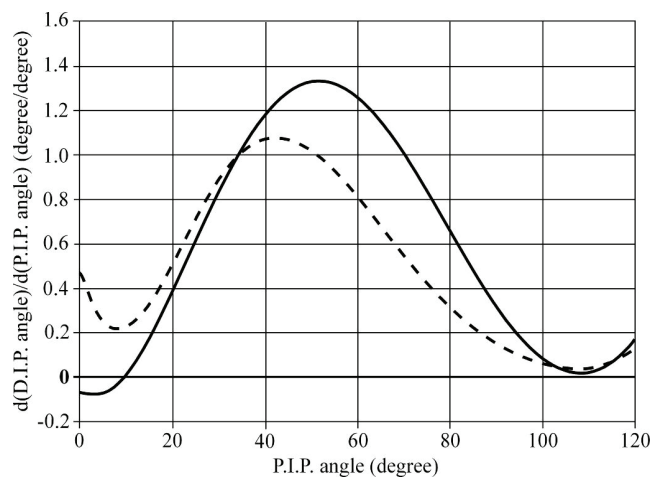

Fig. 5. Calculated derivatives of the analytical fits of the D.I.P.–P.I.P. flexion angles for a V-plus (solid line) and a V-minus (dotted line) finger

Both curves show that in function of the P.I.P. flexion angle the correlation between P.I.P. and D.I.P. flexion displays a variable response of D.I.P. flexion

per degree of P.I.P. flexion angle. This response, however, differs for both cases. In a normal finger (V+) the maximum of D.I.P. flexion per degree of P.I.P. flexion reaches nearly 1.4 degree/degree. In an intrinsic V– finger the maximum reaches only about one degree D.I.P. per degree P.I.P. flexion. Further on for V– the D.I.P. flexion peaks at about 10 degrees lower than the maximum in the normal finger of V+. Not only reaches the maximum of flexion in an intrinsic V– finger only 80% of the maximal flexion of a normal finger, the ability to flex the D.I.P. joint more declines faster than in a normal finger when going to higher P.I.P. values.

4. Discussion

In the anatomy of the finger, the P.I.P. region is a key element in the understanding of the coupling of healthy and pathological finger movements, and in the analysis of the angular correlation between D.I.P. and P.I.P. flexion [16]–[18]. In this region certain bundles of the extensor assembly (i.e., the medial and lateral bundles and the spiral fibers) and the P.I.P. joint curvature are of predominant importance [17], [21].

In every P.I.P. flexion a subsequent, and even simultaneous D.I.P. flexion is enabled by the following mechanism. During P.I.P. flexion the lateral bundles which together constitute the extensor tendon for the D.I.P. joint slide distally, suspended by the spiral fibers, thus allowing correlated D.I.P. flexion. This suspension is well-described [15], [17], [18], [24], as is the interdependence of D.I.P. flexion and P.I.P. flexion [7], [22], [23]. The suspension function of the spiral fibers has recently been recognized and identified by Durand et al. [5], who performed reconstructions of pathologically elongated spiral fibers in a rheumatoid arthritis finger.

Up to now, a mathematical expression of the angular correlation in terms of the above anatomical structures is not known. Therefore we tried a model-wise approach, based on two-dimensional geometrical interdependence in the sagittal plane and numerical values of these structures. To our knowledge, Gaul [6] is the only one who launched a similar approach, limited to one dimension. He describes, as we do, that the D.I.P. flexion is enabled because of the slackening of the lateral bundles under P.I.P. flexion. However, when calculating the angular displacement of the distal phalanx, he only includes the longitudinal component of the lateral bundle displacement into his model, which therefore can be regarded as a first order approximation to our findings. In our model not only the two-dimensional distal displacement of the lateral bundles is included, but assumed to be variable and dependent on the P.I.P. flexion angle are also the spiral fibers length and the curvature radius R of the distal end of the middle phalanx.

Applying the model to a given flexion data set with discrete angles, we adapted the parameters of fiber length and curvature radius to fit the experimental data for each angle. This yielded for both parameters a series of angle dependent values which then were least square fitted to a polynomial in the P.I.P. angle, resulting in an analytical expression for either parameter. Inserting both functions into the geometric model expression, we obtained the dependence of the D.I.P angle on the P.I.P. flexion $\varphi = \varphi(\theta)$ in a closed analytical expression, which closely follows the given experimental data. From this expression the first-order derivative $\varphi' = \dfrac{d\varphi}{d\theta}$ can be calculated analytically.

5. Conclusion

Information on the differences between normal and pathological flexion of fingers, e.g., in the intrinsic-minus hand, also clearly formulated by Scheker [13], is more pronounced and easier accessible from the derivatives of the D.I.P.–P.I.P. flexion behaviour than from the direct angular correlation data. Comparing the first-order derivatives, which give the rate of change of the D.I.P. angles, allows for a better analysis of the situations at hand than comparing the direct angle measurements, which should justify the method proposed here.

Appendix

A.1. Kinematical model of D.I.P.–P.I.P. flexion

The definition of the necessary quantities is shown in Fig. A.1, giving a simplified lateral view of the extensor system with the middle phalanx in its center and the finger under flexion with the angles $\theta \neq 0$, $\varphi \neq 0$.
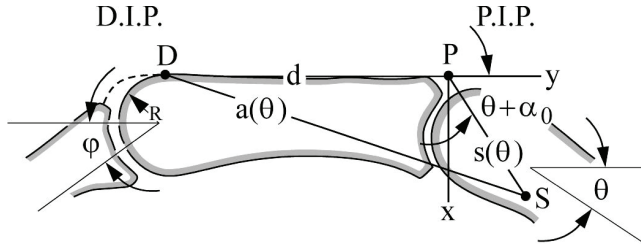
Fig. A.1. Finger extensor assembly schematically
in lateral view

By means of the points D, P and S from Fig. A.1, the length of the distance $a(\theta)$ and the length of the (terminal) spiral fiber $s(\theta)$ can be expressed:

$a(\theta) = $ distance $\overline{DS}$,

$s(\theta) = $ distance $\overline{PS}$.

For the finger in the extended position with the angles $\theta = \varphi = 0$, the distances a and s take on the initial values $a(0)$ and $s(0)$, which are the lengths of the lateral tendon and the terminal spiral fiber, respectively.

The distance d between the points D and P, marking the longitudinal distance between the D.I.P. and the P.I.P. joint at the dorsal side of the finger, is a constant which can be derived from anatomical data.

In the extended position of the finger, the spiral fiber $s(0)$ makes an initial angle α_0 with the reference line.

We assume that for any P.I.P. flexion angle θ the spiral fiber s has rotated around point P over approximately the same angle θ. The spiral fiber thus makes the angle $(\theta + \alpha_0)$ with respect to the reference line. Further on we assume that the length of the lateral part of the spiral fiber $s(\theta)$ changes during rotation and depends on its angular position $(\theta + \alpha_0)$. Also during rotation becomes $a(\theta) < a(0)$, so that a part of the lateral tendon can move distally.

We introduce a right handed Cartesian coordinate system with its origin in point P and its y-axis pointing proximally along the reference line. The lengths $a(0)$, $a(\theta)$ can be expressed by their components a_x, a_y in this axis system. These components are functions of the distance d and the fiber lengths $s(0)$, $s(\theta)$ and therefore depend on the variable θ. They can be derived by applying some simple trigonometry to the situation outlined in Fig. A.1, resulting in the following expressions

$$a(0) = \sqrt{a_x(0)^2 + a_y(0)^2}, \quad a(\theta) = \sqrt{a_x(\theta)^2 + a_y(\theta)^2},$$

$$a_x(0) = s(0) \cdot \sin \alpha_0, \quad a_x(\theta) = s(\theta) \cdot \sin(\theta + \alpha_0),$$

$$a_y(0) = s(0) \cdot \cos \alpha_0 + d,$$

$$a_y(\theta) = s(\theta) \cdot \cos(\theta + \alpha_0) + d.$$

When, in a thought experiment, we tighten a string between the end points P and D, leading it over point S, then in the extended situation its length equals the sum $\{a(0) + s(0)\}$. Under flexion of the P.I.P. joint over the angle θ the string will slacken, because the length $\{a(\theta) + s(\theta)\}$ shortens in comparison with the extended situation. This means that the tendon can glide distally along point D over the distance Δl and lets the distal phalanx rotate around a centre in the distal end of the middle phalanx. The length difference Δl with

$$\Delta l = \{a(0) + s(0)\} - \{a(\theta) + s(\theta)\}$$

("the slackening of the rope") enables D.I.P. flexion over an angle φ according to

$$\Delta l = \varphi \cdot R$$

with R the radius of curvature of the distal end of the middle phalanx. We assume a radius of curvature $R = R(\varphi)$ dependent on the angle φ, and as $\varphi = \varphi(\theta)$, we get $R = R(\theta)$.

We can finally write

$$\varphi(\theta) = \frac{\sqrt{a_x(0)^2 + a_y(0)^2} + s(0) - \sqrt{a_x(\theta)^2 + a_y(\theta)^2} - s(\theta)}{R(\theta)}$$

(1)

with $R = R(\theta)$ and $s = s(\theta)$ to be adapted by a best fit to the experimental data.

A.2. Remark

Neglecting in equation (1) the contribution of the x-components and assuming $R \approx s \approx$ const, we get the expression derived by Gaul [6]

$$\varphi(\theta) = \cos \alpha_0 - \cos(\alpha_0 + \theta). \qquad (2)$$

Equation (2) describes the angular correlation well for small P.I.P. values, but deviates strongly from the experimental data for higher P.I.P. angles.

The assumption $R \approx s \approx$ const is partly confirmed by our results, as we obtain indeed $R(0) = s(0)$, but only for the values near to zero P.I.P. angle.

Acknowledgements

Dr. M. Moens, PhD, neurosurgeon, is explicitly thanked for his initial help in performing measurements. Mr. H.G. Wetselaar, medical artist, and Mrs. M. Ieven, specialised illustrator, are gratefully acknowledged for their work in producing our figures.

References

[1] ABACI T., MORTARA M., PATANÈ G., SPAGNUOLO M., VEXO F., THALMANN D., *Bridging Geometry and Semantics for Object Manipulation and Grasping*, Proceedings of the 1st Workshop towards Semantic Virtual Environments, University of Geneva, Villars, Switzerland, 2005, 110–119.

[2] COLDITZ J.C., ERDMANN D., LEVIN L.S., *Lumbrical tightness: testing and stretching*, J. Hand Surg., 2002, Vol. 27(B, 1), 64.

[3] COLDITZ J.C., *A new method for interosseous muscle elasticity scoring*, J. Hand Ther., 2004, Vol. 17(1), 83–84.

[4] DUMONT C., ALBUS G., KUBEIN-MEESENBURG D., FANGHÄNEL J., STÜRMER K.M., NÄGERL H., *Morphology of the interphalangeal joint surface and its functional relevance*, J. Hand Surg., 2008, Vol. 33(A), 9–18.

[5] DURAND S., GAUJOUX G., MACQUILLAN A., *Triggering of the lateral slip of the extensor mechanism on a Bouchard's node*, J. Hand Surg. Eur. Vol., 2011, Vol. 36(4), 340–341.

[6] GAUL J.ST., 1971. *The ratio of motion of the interphalangeal joints*, unpublished report.

[7] HAHN P., KRIMMER H., HRADETZKY A., LANZ U., *Quantitative analysis of the linkage between the interphalangeal joints of the index finger. An in vivo study*, J. Hand Surg. Br. Eur., 1995, Vol. 20B(5), 696–699.

[8] HAUCK G., *Die Ruptur der Dorsalaponeurose am ersten Interphalangealgelenk, zugleich ein Beitrag zur Anatomie und Physiologie der Dorsalaponeurose*, Arch. Klin. Chir., 1923, Vol. 123, 197–232.

[9] HOLGUÍN P.H., RICO Á.A., GÓMEZ L.P., MUNUERA L.M., *The coordinate movement of the interphalangeal joints: a cinematic study*, Clin. Orthop. Relat. Res., 1999, Vol. 362, 117–124.

[10] LANDSMEER J.M.F., *The anatomy of the dorsal aponeurosis of the human finger and its functional significance*, Anat. Rec., 1949, Vol. 104, 31–44.

[11] MCNAMARA B., *The ulnar nerve*, Adv. Clin. Neurosci. Rehabil., 2003, Vol. 3(2), 25–26.

[12] NAVSA N., *Skeletal morphology of the human hand as applied in forensic anthropology*, PhD Thesis, University of Pretoria, 2010.

[13] SCHEKER L.R., *Reimplantation, transplantation*, Rev. Med. Univ. Navarra, 2003, Vol. 47(1), 12–16.

[14] SCHMIDT H.-M., LANZ U., *Surgical anatomy of the hand*, Thieme, Stuttgart, New York, 2004.

[15] SHOLUKHA V.A., VAN ZWIETEN K.J., LIPPENS P.L., ZINKOVSKY A.V., *Finger tendons kinematics assessing from motion dynamics computer oriented modeling*, J. Biomech., 1998, Vol. 31(S1), 29.

[16] TUBIANA R., *Rappel de l'anatomie de l'appareil extenseur des doigts au niveau de l'articulation interphalangienne proximale*, R. Tubiana, Traité de chirurgie de la main, Tome 3, Paris, Masson, 125–128.

[17] TUBIANA R., *Anatomy of the extensor apparatus at the level of the proximal interphalangeal joint*, R. Tubiana, The Hand, Volume III, Philadelphia, PA, W B Saunders Co., 1988, 101–105.

[18] TUBIANA R., THOMINE J.-M., MACKIN E., *Examination of the hand and wrist*, 2nd edition, Martin Dunitz, London, 1996.

[19] VAN DER MEULEN J.C., *Causes of prolapse and collapse of the proximal interphalangeal joint*, The Hand, 1972, Vol. 4(2), 147–153.

[20] VAN ZWIETEN K.J., *The spiral fibers (Hauck) in the extensor assembly of the human finger*, Acta Morphol. Neerl. Scand., 1978, Vol. 16, 143–144.

[21] VAN ZWIETEN K.J., *The extensor assembly of the fingers in man and non-human primates: a morphological, functional and comparative anatomical study*, PhD Thesis, University of Leiden, 1980, J. J. Groen en Zoon, Leiden.

[22] VAN ZWIETEN K.J., POTEKHIN V.V., LIPPENS P.L., SHOLUKHA V.A., SCHMIDT K.P., ZINKOVSKY A.V., *The influence of finger position on percussion sounds*, Proceedings of the 13th International Congress on Sound and Vibration (ICSV 13), July 2–6, 2006, Vienna, Austria. Eds.: J. Eberhardsteiner, H.A. Mang, H. Waubke. Vienna University of Technology, Austria.

[23] VAN ZWIETEN K.J., LIPPENS P.L., GELAN J., ADRIAENSENS J., SCHMIDT K.P., THYWISSEN C., DUYVENDAK W., *Coordination of interphalangeal flexion in the human finger*, J. Hand Surg. Eur. Vol., 2008, Vol. 33(1), 170–171.

[24] ZANCOLLI E.A., COZZI E.P., *Atlas of surgical anatomy of the hand*, Churchill Livingstone, New York Edinburgh London, 1992.

[25] ZUMHASCH R., WAGNER M., KLAUSCH S., HIRT B., *Anatomie und Biomechanik der Hand*, 2. Überarbeitete Auflage, Thieme Verlag, Stuttgart, 2012.